Journal of Architectural Conservation

ISSN: (Print) (Online) Journal homepage: www.tandfonline.com/journals/raco20

Electrical resistivity tomography of a masonry bridge: assessing water infiltration on Prebends Bridge, Durham, UK

L. Jones, J. Jenkins, L. Foltier & S. Nielsen

To cite this article: L. Jones, J. Jenkins, L. Foltier & S. Nielsen (09 Jul 2024): Electrical resistivity tomography of a masonry bridge: assessing water infiltration on Prebends Bridge, Durham, UK, Journal of Architectural Conservation, DOI: 10.1080/13556207.2024.2357501

To link to this article: https://doi.org/10.1080/13556207.2024.2357501

JOURNAL OF ARCHITECTURAL CONSERVATION
https://doi.org/10.1080/13556207.2024.2357501

Electrical resistivity tomography of a masonry bridge: assessing water infiltration on Prebends Bridge, Durham, UK

L. Jones[a], J. Jenkins[b], L. Foltier[b] and S. Nielsen [b]

[a]Natural Sciences, Durham University, Durham, UK; [b]Earth Sciences, Durham University, Durham, UK

ABSTRACT
Non-invasive imaging methods are a useful tool in informing conservation actions for historical buildings. Electrical Resistivity Tomography (ERT) is widely used in geophysics to image the subsurface but has been seldom used for non-invasive imaging of small-scale masonry structures. Here, we propose an adaptation of the method allowing non-damaging investigation of larger-scale stone structures. We report results of an ERT survey of Prebends Bridge in Durham, a heritage masonry structure constructed in 1778. Our assessment is based on data acquired on the paved top surface of the bridge, which is subsequently modelled and inverted with the use of open-source software. Final images of the internal structure of the bridge reveal areas of lower electrical resistivity, that we interpret as representing regions of water saturation. Locations of low resistivity areas are in good agreement with the structural defects and patches of seepage observed externally. These results will help inform remediation work, to preserve this historical structure from further water damage. In future studies, time-lapse imaging may help to highlight water pathways unambiguously (through comparison of dry/wet periods), while additional electrode arrays installed on the sides/base of the structure could be used to better constrain 3D internal structure.

ARTICLE HISTORY
Received 5 April 2024
Accepted 16 May 2024

KEYWORDS
electrical resistivity tomography (ERT); stone; masonry; water infiltration

1. Introduction

Geophysical Electrical surveying provides a powerful non-destructive imaging tool, which is widely applied in archaeological, environmental, geological and engineering applications to assess subsurface structure. Injecting electrical currents into the ground and measuring electric potential differences allows identification of materials with contrasting electrical properties (e.g. soil/rock, dry soil/wet soil, etc.). Over the last several decades, researchers have started to explore the potential of electrical surveying for the assessment of internal structure on a small-scale within masonry structures, such as walls and pillars (see review in[1]). This is particularly relevant to heritage structures

CONTACT S. Nielsen stefan.nielsen@durham.ac.uk
Supplemental data for this article can be accessed online at https://doi.org/10.1080/13556207.2024.2357501.

suffering long-term deterioration linked to water infiltration, where saturated internal areas can be identified by low electrical resistivity anomalies.

Here we explore the potential to scale-up this technique for use on heritage masonry bridges. As a pilot-case we use electrical imaging to assess water infiltration on the eighteenth century Prebends Bridge, in Durham, NE England, which forms part of the Durham World Heritage Site. With simple adaptations to standard survey design and data analysis procedures, we demonstrate the potential of electrical imaging for use in assessing internal structure within heritage masonry bridges.

Below we introduce Prebends Bridge in detail (section 2), before outlining the basic theory of geophysical electrical imaging, and its uses to date in assessing heritage masonry structures in sections 3.1 and 3.2. A full outline of our survey design and analysis are outlined in section 3.3 and 3.4, with resulting images of internal electrical properties of Prebends Bridge displayed in section 4. Finally we interpret our results and discuss how electrical imaging can be optimised and developed further for large scale surveying of masonry bridges and similar structures in section 5.

2. Study site: Prebends Bridge

Prebends Bridge is a Grade I listed scheduled ancient monument located just outside of the Watergate on South Bailey in Durham City Centre, Northeast England, (highlighted in yellow Figure 1a). Its construction was completed in 1778, and it was partially restored in 1955–56.[2] The bridge is built from a locally sourced Carboniferous Sandstone of the Pennine Middle Coal Measures Formation, thought to have been quarried from the rocky promontory on its Eastern side upon which Durham Cathedral sits.[3]

Figure 1. (a) Aerial view of Prebends Bridge (yellow) connecting Durham city centre and the promontory on which Durham Cathedral (red) is located to the rest of the city across the river Wear. Inset map shows locations in NE England. (b) Image showing dimensions of Prebends Bridge (looking NNW), with the Eastern arch (the focus of this study) labelled. (c) Image highlighting structure of the bridge deck looking ENE. Photographs in b and c sourced from, taken by Alan Marsh.

Note: Historic-England, National heritage list: Prepends bridge listing 1121354 (2024). Available at https://historicengland.org.uk/listing/the-list/list-entry/1121354.

The bridge is supported by piers 15 m above the river Wear and comprises three stone arches spanning a distance of ~70 m, Figure 1b. Abutments rise upwards into the steep banks on either side of the river. An asphalt road runs along the bridge deck bordered by 1 m wide pavements formed of sandstone flag and kerbstones, with a parapet running along the bridge edge, Figure 1c. Six gutters extend through the parapet on each side of the bridge to external gargoyles, located at 3 m offsets on either side of the arch keystones (Figure 2c).

Plans from engineering work that took place on the bridge deck in the late 1980s (confirmed with a 2010 trial pit located within roadway, as marked on Figure 2c),

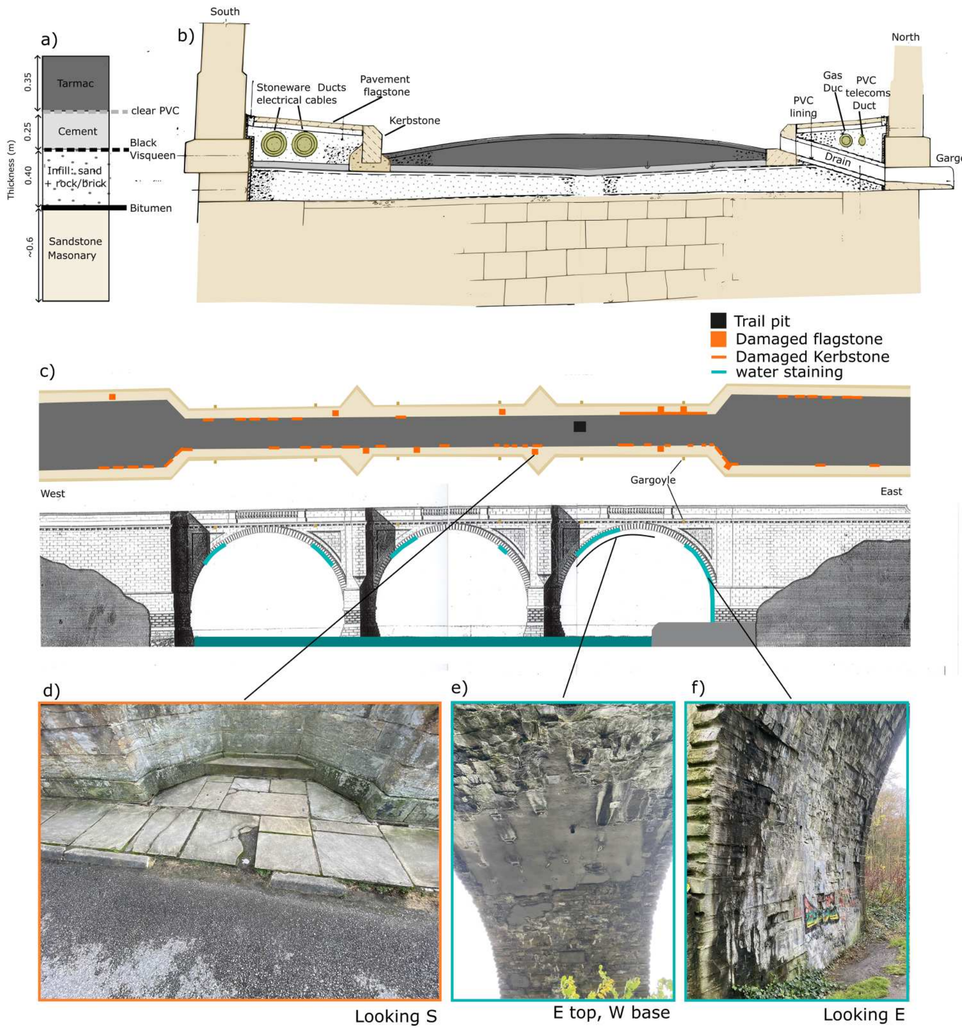

Figure 2. (a) Scaled log of Prebends Bridge internal structure, observed in trail pit within the centre of tarmacked road based on details from, pit location shown by black square on c. (b) Cross-section of Prebends Bridge internal structure, adapted from provided by Historic England via Durham Cathedral. (c) Architectural drawing of bridge side view and deck plan (adapted from), with areas of damaged paving and kerb stones highlighted in yellow as identified by. Source: A. March, *Prebends Bridge*; R.T. James and Partners, *Prebends Bridge: Existing and proposed cross-section. drawing number: 12626n/3* (1987); The Morton Partnership Ltd., *Structural assessment report of Durham Cathedral.*

suggest an internal structure as displayed in Figure 2a. This consists of ≈35 cm tarmac underlain by a 25 cm thick steel-mesh-reinforced concrete slab encased between layers of PVC, above a layer of backfill comprised of mixed dark grey/black silty sand, domestic ash, clay bricks and sandstone fragments.[4] Beneath the fill material, a layer of bitumen coats the stone masonry of the bridge. Beneath the pavement flagstones, infill material surrounds services pipes/ducts, which are again underlain by PVC lined concrete.

Water infiltration and subsequent deterioration of the external stonework has been observed for several decades. This poses a hazard to the small number of boats passing beneath the bridge on the river, and to a greater degree for pedestrians using the footpath that passes beneath the eastern arch (Figures 1b and 2c). Remedial work to the worst affected areas which were identified on the underside of the eastern arch took place in 2011, with areas of concrete filler patch repairs (e.g. as seen in Figure 2e) and insertion of washer plates and rods into areas of significantly eroded masonry. However a subsequent engineering survey in 2021, noted areas of stone work adjacent to the concreted repairs, exhibiting saturation, water staining and algae growth,[5] indicating that water infiltration is still ongoing, though redirected to alternate paths around cemented regions.

3. Methods

Electrical surveying has the potential to identify water-saturated regions within the structure of Prebends Bridge (as areas of low electrical resistivity). If areas of surface ingress and infiltration pathways through the structure can successfully be identified, this can direct where future re-waterproofing work needs to be focused.

3.1. Basic principles of electrical resistivity tomography

Measurements of a material's apparent electrical resistivity can be made using a simple circuit consisting of a power source, a volt meter and four electrodes. Two current electrodes (C1, C2) act as a current source and current sink, while the electrical potential (voltage) is measured between two voltage electrodes (P1, P2). With known input current I and measured voltage V, it is possible to calculate an electrical resistance $R = V/I$. The electrodes can be moved to acquire measurements at different positions. Rather than moving the same four electrodes for each new reading, an array of more electrodes can be installed and connected to a multiplex cable, where different groups of 4 electrodes are selected for each reading.

Since current flows through a volume of material in the subsurface rather than across a simple circuit, the resistance measured from current and voltage is converted to an apparent resistivity ρ (units of Ω m) by multiplication with a characteristic length of the electrode acquisition system. The specific equation used to calculate resistivity from resistance depends on the array configuration, but is generally proportional to the spacing between electrodes. For example, in the widely used *Wenner* configuration, the four electrodes are aligned in the sequence (C1, P1, P2, C2) and the spacing a between two successive electrode is constant (Figure 3(a)); in this case $\rho = 2\pi aR$.

To build a 2-dimensional model of subsurface electrical properties (a tomographic image), a four electrode spread with constant spacing is moved by steps along a transect,

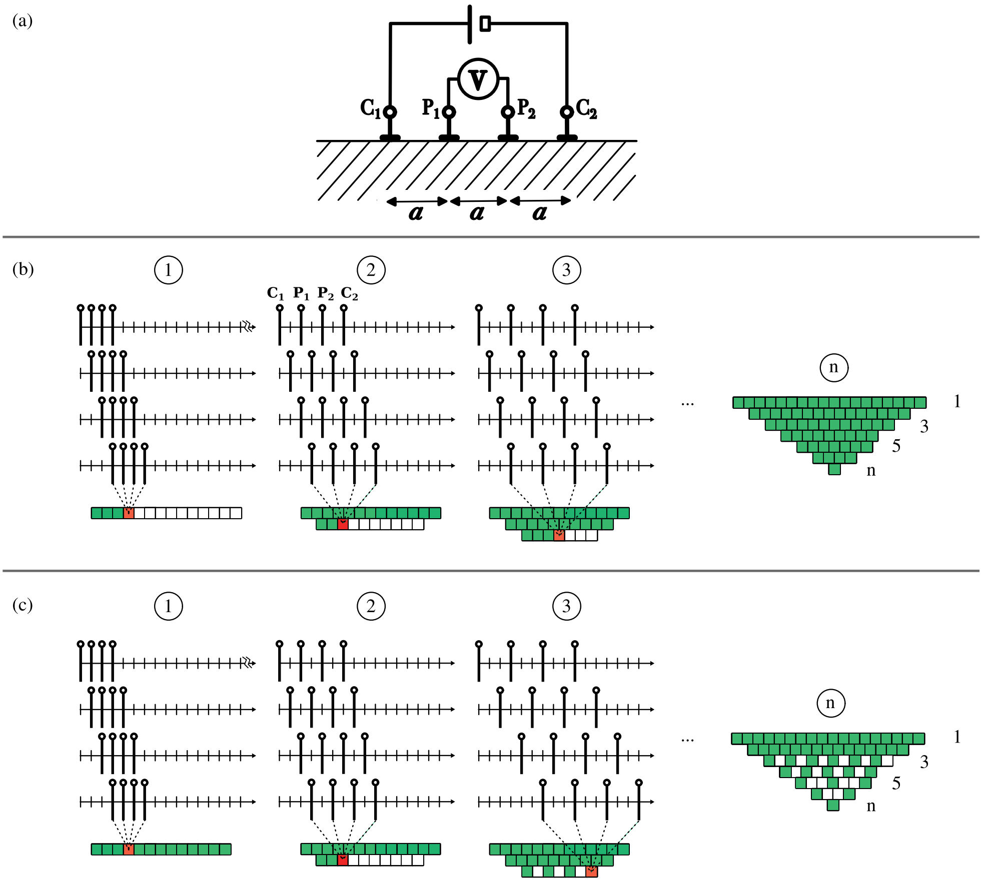

Figure 3. Configuration of electrode positioning in electrical surveying. (a) Classic Wenner electrode array configuration with two outer current electrodes (C_1, C_2), two inner potential electrodes (P_1, P_2) with constant spacing separation *a*. (b) Conventional marching scheme (also used in the automated multi-electrode system) where the Wenner array is used to take *n* readings with different centre points and different spacings *a*. The acquisition for the first 3 levels is illustrated (pins with round heads represent electrodes). An illustration of the final pseudo-section obtained for n levels is shown right (in the example n = 7). (c) Sparse marching scheme, used in our survey of Prebends Bridge. Time-efficiency is gained by skipping steps at deeper levels of acquisition. In this example, steps at levels 1 and 2 correspond to the initial electrode spacing *a*. Starting from level 3, steps are increased to 2a, and from level 5, to 3a (and so on for arrays of greater length than illustrated example). The resulting pseudo-section (right) is sparser at depth.

taking a measurement at each step, and producing a line of measurements with a similar depth sensitivity (Figure 3b-1). The spread is then returned to the start of the transect, and the along-transect swipe is repeated, but with an increased electrode spacing to allow a greater depth penetration (Figure 3b-2). Repeated swipes at ever increasing electrode spacings along the same transect (Figure 3b-3) allows the building up of a 2D section of apparent resistivity referred to as a pseudo-section. As the spacing increases, fewer combinations of electrodes can be utilised, thus the number of readings decreases as the depth (Figure 3b-4). Before being transformed into a 2D model, the raw measurements can be plotted in an inverted-pyramid (pseudo-section) for a preliminary inspection. To a trained eye, the initial pseudo-section may help form a preliminary idea of the resistance distribution.

However, the path and penetration depth of the current following between electrodes depend on the inhomogeneous distribution of resistivity in the sub-surface. Thus each measurement will integrate a variable resistivity within a sampled volume, preferentially sensitive to areas traversed by more current. As a consequence the raw data (apparent resistivity) is difficult to interpret, and careful modelling paired with misfit minimisation techniques are required to construct a reliable image of the true resistivity distribution. In geophysics, this procedure is generally referred to as inverse modelling. With measurements usually confined to the surface such problems can lead to a mathematically ill-conditioned, ill-posed or mixed-determined problems, with consequent issues such of non-uniqueness (multiple models may fit the data equally well) or excessive sensitivity to noise in the data. These are common problems across many geophysical subsurface imaging techniques, but they can be mitigated by imposing model regularisation during the inverse process. Regularisation allows the retention of a limited number of models that show user-defined desirable or realistic features, and attributes less weight to model parameters that are poorly constrained.

3.2. Previous use of electrical surveying for assessing heritage masonry

In the 1990s several researchers began exploring electrical surveying for imaging the interior of masonry structures, demonstrating its effectiveness at identifying areas of internal deterioration that are often non-obvious based on a structure's superficial appearance.[6,7] Since these early investigations electrical surveying has proved an effective tool for assessment of crack distribution,[8] monitoring of grouting injection[9] and identifying the distribution and movement of moisture[10,11] within small-scale heritage masonry structures.

These studies have highlighted several key adaptations to standard surveying techniques that need to be considered when applying this technique to heritage architectural features:

- Geometrical shape of surveyed structures: This is not usually considered beyond inclusion of variable surface topography for more common subsurface surveys where the model depth is generally limited only by the sensitivity of data, rather than a 3D shape.
- Electrode attachment: Standard surveys use ~30 cm long metal probes directly buried in the ground. While some previous heritage masonry studies use metal nails directly inserted into surfaces[12], in many cases this semi-destructive approach is not appropriate, and others have explored the use of medical electrocardiogram electrodes as an alternative.[13,14,15]

To date, investigations have been limited to small-scale (several meters) studies of walls and columns, with only one known application to a small heritage masonry bridge (9 m long × 3 m high).[16] In this work we explore how electrical resistivity tomography (ERT) imaging can be scaled up to larger investigations to assess the highly variable geometry of masonry bridge structures over the scale of tens of meters.

3.3. Prebends Bridge electrical survey design

On Prebends Bridge, electrical surveying was carried out over the eastern arch –a region with observed water damage and the site of previous repair attempts (Figure 2e,f) – with the aim of mapping water infiltration pathways. Surveys took place over the course of several weeks in July–August 2023. This was a wet period of the summer, with rain occurring most days. While measurements were only undertaken when the bridge surface was visibly dry, it is assumed that any internal material subject to water infiltration would have remained saturated for the whole period, due to persistent re-wetting. This was confirmed with consistent repeated measurements on different days across the same area. Two 25 m long survey lines were located along the sandstone pavements on either side of the eastern arch, with an additional line extending onto the abutment, as shown in Figure 4(a). Readings on the tarmac road running along the centre of the bridge were not possible owing to the large resistivity of the surface layer. Two different acquisition strategies were used as described below.

Simple Wenner. A Wenner array of 4 electrodes was moved laterally by *steps* along survey lines (highlighted in red on Figure 4a). The same transects were repeated with different electrode *spacings* to produce a number of *levels* of increasing penetration depths (Figure 3b). The electrode spacing varied from 0.2–2.8 m. The steps between measurements was 0.2 m for the first two levels, but were doubled every other level, resulting in a more time-efficient *sparse* marching scheme (Figure 3c). This efficiency comes at the cost of a lower horizontal density of data points at deeper levels of the pseudosection; however this loss of data was considered justified by the fact that wavelength of the resolved structure at deeper levels is lower in any case. Electrodes were connected to a Terrameter instrument, with four voltage readings taken at each measurement point to ensure consistency and allow error estimation. For a more efficient acquisition, the electrodes were placed within to static plastic bar, with holes for different spatial positioning, to allow for a variable the electrode spread (as shown in Figure 4b). Several poles were attached on-end to increase the electrode spacing as needed. This allowed all four electrodes to be moved together while maintaining a constant spacing between them, accordingly we refer to this as a permanent spacing device (PSD).[17]

Multiplex Wenner. We also explored use of an automated TIGRE acquisition apparatus (shown in Figure 4c) which uses multiplex cables to facilitate automated switching of the four electrodes among 64 different positions. A survey was carried out using this equipment along the transect highlighted in blue on Figure 4a. We note that, surprisingly, the use of Multiplex Wenner was not significantly faster or more efficient than manually moving the four electrodes in a simple Wenner configuration within our PSD and taking Terrameter readings by hand. The Multiplex took longer to install and needed to run for a relatively long time (∼3 h) to acquire all the readings. In addition the multiplex system is of considerable weight (particularly the cables) and required transportation, while the simple Wenner could be carried by hand by a single operator. We conclude that, due to its relative agility, the efficient use of a PSD for moving electrodes along the transect, and the insignificant difference in the duration of the two acquisition strategies, the simple Wenner adaptation described here is currently superior to a standard multiplex system for the type of survey that we illustrate.

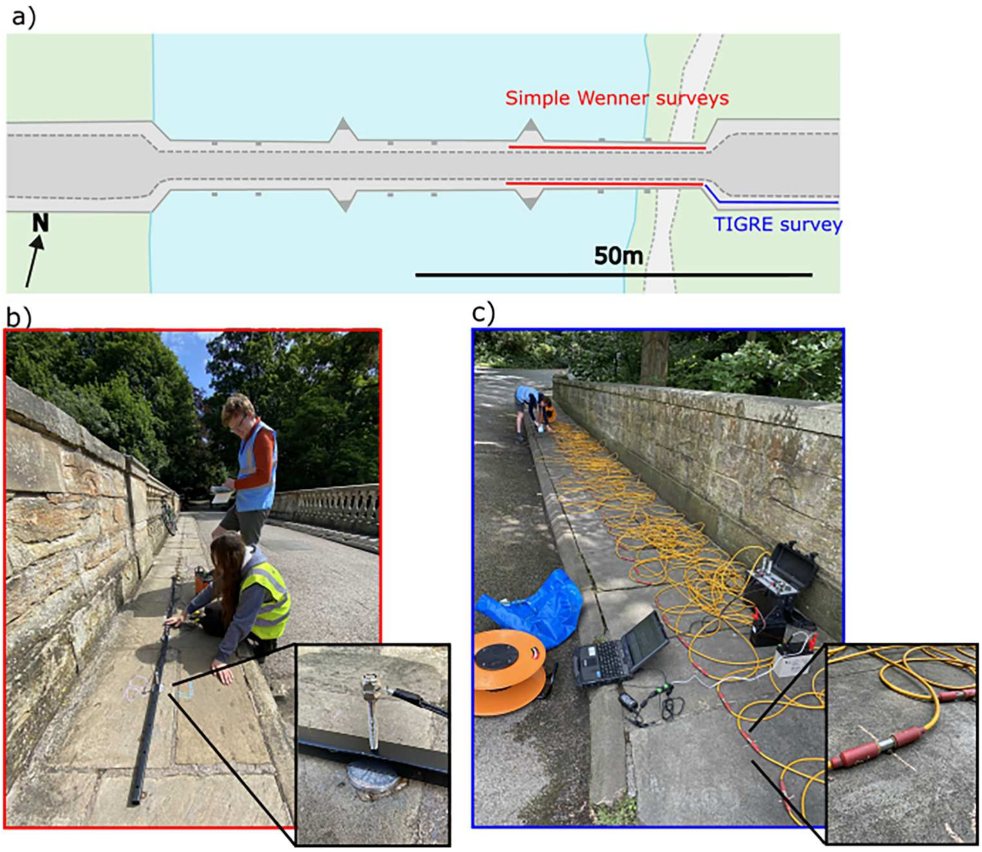

Figure 4. (a) Plan of Prebends Bridge showing location of electrical survey transects for: the simple Wenner approach (red) – two 25 m long transects located on northern and southern pavements over the bridges Eastern arch, and using the TIGRE array (blue), one 15.75 m long transect over the eastern abutment southern side. (b) Photograph of Wenner survey set up, with metal plate electrodes affixed with electrolyte gel (inset), positioned within a PSD which was manually moved along the survey line, with measurements recorded by a Terrameter instrument. (c) Photograph of multiplex survey setup, with metal contacts of cable affixed directly to surface with electrolyte gel (inset) and measurements automatically recorded by a TIGRE instrument.

3.3.1. Electrode design

As outlined above, a key adaptation required for use of electrical surveying on heritage masonry is attaching electrodes to the surface in a non-destructive way that reduces contact resistance sufficiently to allow current to penetrate. We experimented with several options to optimise survey design for use over larger scales than has previously been utilised.

3.3.2. Medical gel pads

Initially wires were directly affixed onto medical electrical adhesive gel pads, which were adhered to the bridge surface for each measurement. While these were initially successful, electrodes quickly became covered in grit and dust, as pads were moved across the transect to cover different positions along the 25 m long survey line. As this build-up of dust and small rubble prevented a good electric contact, the pads required repeated cleaning and eventually removal of the adhesive gel layer. In previous studies[18] a larger number of small medical ECG gel pads were used successfully, by fixing them in position and covering all possible electrode locations, avoiding the issue of dirt build up on moving. In our case fixed positions were less viable, due to the larger scale and number of datapoints included in the survey which took place in an area with ongoing pedestrian traffic.

3.3.3. Metal plate electrodes with electrolyte gel

We also designed an alternative electrode type, consisting of a metal disk which was put in direct contact with the rock surface with a thin layer of electrolyte gel to facilitate current flow (as shown in Figure 4b – inset). Electrodes sitting within our PSD, included a spring component, such that the four points could accommodate a small amount of surface topography across the array, caused by uneven paving. Electrolyte gel proved effective, requiring replacement every 3–4 measurements. Small amounts of the water-based gel residue are left on the surface, which are quickly naturally removed by weather, or could be manually washed away if necessary. A similar approach was using a multiplex cable and an automated TIGRE instrument, using electrolyte gel to place metal sections of the multiplex cable in direct contact with the stone surface (Figure 4c – inset). While this provided effective current penetration, the non-fixed nature of contact points meant this was impractical, particularly on a public thoroughfare, since a slight movement of wiring could disrupt contact.

3.4. Inverse modelling and data analysis

3.4.1. Inversion approach

As outlined in section 3.1, raw (apparent resistivity) data is difficult to interpret without further analysis. In order to generate a realistic model for the true resistivity throughout the depth of the bridge, the four readings taken at each measurement point were averaged and then used as inputs (along with associated standard errors)for inverse modelling using the Python Geophysical Inversion and Modelling Library (pyGIMLi).[19] This inversion strategy consists of an error-weighted minimisation procedure, using a Gauss–Newton algorithm to perform an iterative least squares fit, which identifies a best-fitting model that can reproduce input data. The modelling procedure requires definition of a model mesh within which varying subsurface electrical properties are determined during the inversion process, while model selection is constrained based on user-set regularisation parameters.

3.4.2. Mesh design

In the standard operating procedure of pyGIMLi codes, a polygonal mesh is automatically constructed based on the positions of the electrodes, to define an unstructured rectangular area of user-defined finite depth. However, specific meshes can be designed if needed, usually to allow incorporation of surface topography when electrode positions are not at equal elevation.

In our case, a two-dimensional structured polygonal mesh was designed to capture the geometry of the arches in the lower part of the model, imposing fixed model boundary conditions based on the bridge's true structure. Architectural drawing of the side of the bridge (adapted from figure in[20] provided by Durham Cathedral) and measured electrode positions were used to produce the mesh shown in Figure 5, which we use in our data inversions. Consideration of the impact that the use of a structured geometric vs unstructured mesh has on results is considered in the Discussion (section 5).

3.4.3. Regularisation

pyGIMLi software allows users to impose a number of different common regularisation techniques that reduce the sensitivity of the model to noise within the data, such as first or second order smoothing (minimisation of the model gradient or curvature) or damping (favours models with bounded parameter values, i.e. solutions that do not diverge form the minimum norm model). Tests show that inversion results are not hugely affected by the type of regularisation chosen, thus we apply the software default of 1st order smoothing. The relative strength of the regularisation is controlled through selection of a parameter (λ), the value of which is set prior to running the inversion.

Identifying an optimal λ value is non-trivial; strong regularisation (large values of λ) produce very smooth models which may hide important physical features, while excessively weak regularisation (small λ) produces strong amplitude, small-scale variations within the model which are likely to be nonphysical. To select a reasonable λ for each transect, a range of regularisation strengths were tested in the inversion process and the cumulative misfit (defined by the Chi-squared statistic) for resulting model was calculated. These were compiled and plotted as a trade-off curves, an example of which is shown in supplemental Figure S1. From these, appropriate ranges of regularisation strength could be determined, based on identifying the knee of the curve where misfit is minimised. A value of $\lambda = 30$ was selected and used to produce the final models shown in the results section, as this value fell near the minimum of the trade-off curve for both transects.

3.5. Model resolution

To appraise the resolution of our modelling results we conducted a number of numerical tests using known input checkerboard resistivity patterns of varying

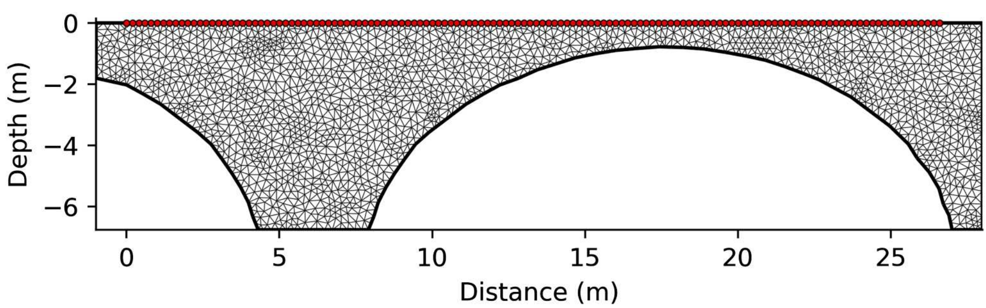

Figure 5. The polygonal mesh used to carry out the pyGIMLi modelling and inversion. The mesh was designed to reproduce the boundary conditions imposed by the bridge's geometry, including the arches, and the positions of the electrodes on the surface (red dots), which must fall on polygon nodes. We note that this 2D mesh geometry neglects variation in the third dimension (across the bridge's width).

dimensions. These were used to simulate synthetic data which was then inverted using the same scheme as for the real data. The results are presented in supplemental Figures S2–5. These reveal that data has the ability to resolve structures of down to 0.5 m in width, and that model depth resolution is dependent on size of imaged structure, with larger features observable to greater depths – the depth resolution limit is roughly equal to the feature size, or half-wavelength of the pattern. Importantly, the checkerboard tests also demonstrate that the sparse marching scheme we use for data sampling is not significantly worse at resolving structure than a full data collection strategy.

4. Results

Figure 6 shows modelled outputs over the northern and southern transects of Prebends Bridge eastern arch (locations in Figure 4a).

4.1. Northern transect observations

On the northern transect (Figure 6a) beneath some superficial high resistivity values in top tens of cm, lies a near continuous band of low resistivity material ($<$ 900 Ohm m) to depths of $\sim$0.5 m, beneath which high resistivity material ($>$ 900 Ohm m) is seen to depths of 3–4 m – the approximate limit of data sensitivity. Two notably high resistivity sections coincide with the underside of the arch at 12 and 22 m along the transect. These are coincident with concreted areas from previous conservation efforts (as shown in photo in Figure 2e). Beneath the apex of the arch, at 17 m along the transect, the shallow region of low resistivity appears to extend to the base of the arch, around the area of the keystone. This area is not concreted on the underside and is coincident with a broken paving tile on the pavement of the bridge deck at the time of surveying. Another low resistivity region on the arch underside at $\sim$23 m along transect was coincident with an area of visible damp above the pedestrian footpath at the time of survey.

4.2. Southern transect observations

In comparison the southern transect (Figure 6b) does not show a coherent low resistivity layer within the top 0.5 m, though disconnected patches of lower resistivity are clearly still present in this depth range. Superficial low resistivity regions can be correlated with notable features on the bridge deck that were observed while undertaking the survey, including the presence of the drainage gutters (in one case partially blocked with vegetation), and broken paving stones or kerbs. Notably low resistivity values persist below 0.5 m, and in several regions are observed at the base of the model on the underside of the arch (e.g. at 4,17,20 and 23 m). The region at 23 m was coincident with an area of visible water staining and damp observable on the underside of the arch adjacent to a concreted region. We note that there no clear low resistivity path between this region and the bridge deck.

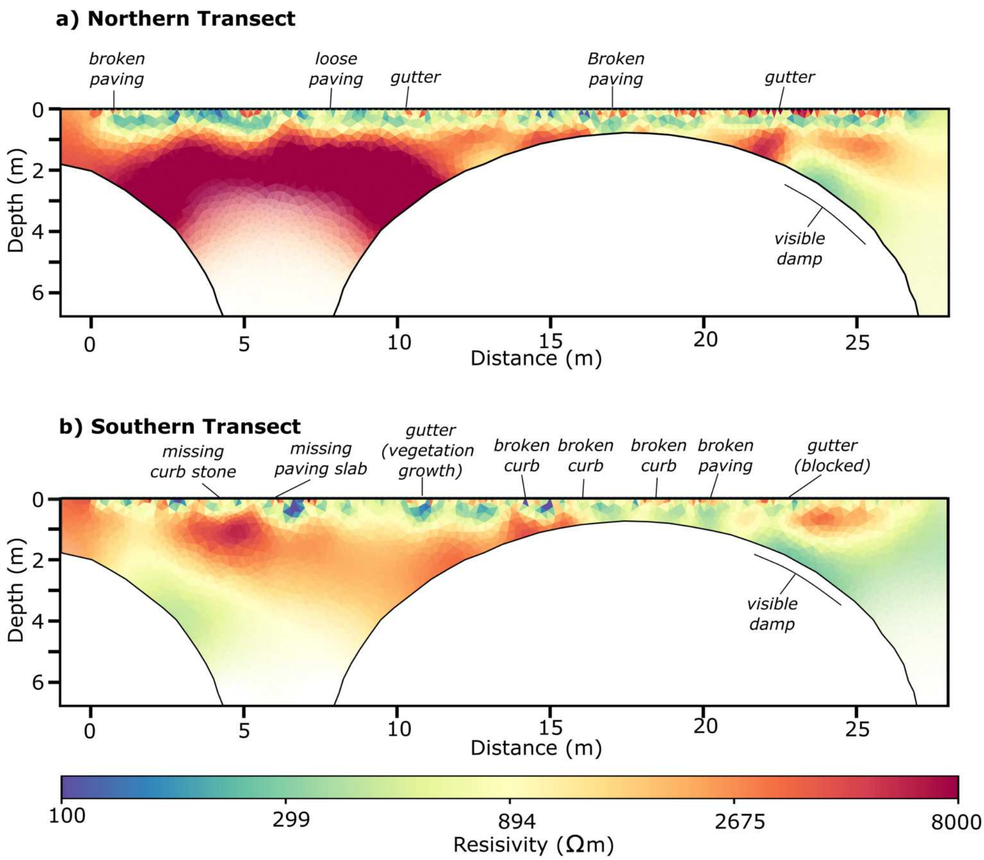

Figure 6. Modelled outputs of the internal electrical resistivity structure over two transects of Prebends Bridge's eastern arch. (a) Shows the northern transect and (b) shows a southern transect. Notable superficial features observed at the time of surveying are labelled.

4.3. Interpretation

The 0.5 m thick low resistivity region at the top of both transects, coincides with the depth to a reinforced concrete slab encased at top and bottom with layers of PVC plastic, as shown on structural plans of the bridge (Figure 2a). Beneath the sandstone paving stones, this region contains services (electrical power lines on the south side, and a gas duct on the north side) surrounding by fill material (sand, ash and masonry fragments). Our results suggest that infill material beneath much of the pavement becomes saturated after rainfall (leading to low resistivity values), with infiltration likely facilitated by numerous cracked flags and kerbstones observed on the bridge deck. This is consistent with an engineering study in 2010, which noted damp fill material beneath paving tiles around drainage regions.[21] However the waterproof layer provided by the concrete PVC-line slab appears to effective in shielding deeper bridge structures across much of the region on the northern side of the bridge, but is apparently significantly less effective on the southern side. This was visually confirmed when subsequent work in the days after the survey, lifted pavement flag stones to reveal saturated infill material (supplemental Figure S4).

Low resistivity on the arches suggests that in some places water infiltrates through the entire structure, due to the permeability of the sandstone the bridge is built from. This also suggests the effectiveness of the bitumen water-proof coating to the stonework beneath the final layer of infill (Figure 2a), is compromised. Clearly affected regions are located over the keystones on both sides of the bridge, where low resistivity pathway can be observed directly between the surface and underside of the arch. For some other regions no clear water pathways from surface to saturated areas are apparent (such as the southern side anomaly at 4 m along transect). This suggests the 3D flow of water through the bridge structure, which it was not possible to fully map out due to the highly insulating tarmacked road surface which does not allow electrical surveying. The observation of low resistivity saturated regions around concreted repairs to the underside of the arch highlight how these attempts have redirected the flow of internal pathways, rather than addressed the root cause of the problem. We also note that the southern transect shows lower resistivity values on the arch underside compared to the northern transect, and that both gutters on this side of the bridge were observed to be blocked. This suggests a lack of efficient water drainage from the bridge deck may be aggravating water penetration here.

5. Discussion

As noted by,[22] moisture is a key factor in building stone decay, both directly (through dissolution and direct transformation of rock constituents) and indirectly (influencing salt dissolution/crystallisation and biological decay). Thus, imaging internal water pathways is crucial to understand and monitor ongoing deterioration in heritage structures, to allow design of appropriate interventions, and test their effectiveness. For heritage masonry bridges this is particularly relevant, given many are still used by both pedestrian and road traffic, or even supporting trainlines (e.g. Ribblehead viaduct in Yorkshire). While modelling based desk studies such as,[23] have indicated the potential effectiveness of using electrical imaging methods on heritage masonry bridges, little work has explored the logistics of implementing this in practice.

Our test-case study on Prebends Bridge in Durham and the mapping of damp regions within it, suggests this is easily achievable, with simple adaptations to standard surveying techniques coupled with the use of modern inversion software (as discussed in section 5.1). Our results indicate past interventions which concreted sections of the arches underside, were not effective, acting only to divert water flow around them. Broken flagstones and missing kerb stones provide clear entry for water into the bridge, and internal waterproofing is not entirely effective in preventing deeper penetration. Since this study was conducted (between 18 July and 1 September 2023), the entire length of the northern surveyed transect has been taken up and repaved over the course of September–October 2023. Future studies could test the effectiveness of this measure, by contrasting the re-paved northern side with the southern side.

5.1. *Electrical survey adaptations for use on large scale heritage structures*

Non-destructive electrodes. Partially destructive electrode connections, such as the use of nails or drilled-in metal pins usually relied open to provide a good connection, are not usable on scheduled monuments such as our study site. For smaller-scale (several meter) surveys,[24, 25] clearly demonstrate the effectiveness of using static medical electrical pads in this context. However our study demonstrates that for larger-scale surveys requiring the movement of electrodes along the survey length (or in areas where it is not possible to leave static electrodes long term without disturbance), this becomes impractical, due to dirt build-up interfering the effectiveness of electrode contact. For moveable surveys flat metal probes which are periodically re-moistened with a thin layer of electrolyte gel (easily removed by washing off with water) proved more effective. The strategy of using a spring-loaded PSD[26] was also key in producing good contact between electrodes and the bridge surface, while allowing for small degree of topography due to uneven flagstones.

Realistic geometric model set-up. Early studies investigating the use of electrical imaging on heritage masonry structures noted the significant impact that 3D geometry could have on modelled results.[27] Quantification of these effects showed that not considering 3D geometry could lead to inaccuracies in modelled resistivity values, affecting areas up to several meters within the structure.

The variable thickness of material over the bridge arches is an important structural factor to consider when imaging the resistivity variations. The lateral walls of the bridge may also influence the resistivity readings. However, the walls are essentially planar, vertical and parallel to the transect (to a first approximation), therefore associated edge effects are likely to have reasonably consistent impacts throughout the model (based on modelling results of [28]) and impact only absolute values of resistivity measured. They will affect in a lesser way the relative lateral variations of resistivity, that in our case provide more important evidence of water pathways than absolute values. The only region where this assumption is less justified is in the first 10 meters of transects, where they cross a bridge pier, and the very end of transect lines, where slightly wider abutments protrude from the otherwise planar sides of the bridge (Figure 4a).

Accordingly, our modelling assumes a 2D geometry, not accounting for the 3D limits of the bridge sides. In the case of Prebends Bridge (and bridge structures more generally), the $\sim$ 5.5 m wide structure makes it likely that only the closest edge to each transect is likely to significantly impact results. Correlation of results on the underside of arches with externally visible sections of concrete repairs/damp also provides confidence in the robustness of our results using a 2D modelling set-up.

Although both 2D and 3D modelling can be implemented using standard inversion software such as pyGymli,[29] extending to 3D requires significantly more complex adaptations. The computational times would increase and a considerably larger number of model parameters would be inverted, which, in turn, would call for the acquisition of a larger data set with more complete electrode coverage. Thus if a simplified 2D geometry can be justified for use on heritage bridge structures (as appears to be the case here), it significantly increases the ease of implementation and could encourage uptake of this method more widely.

In our study we design a 2D polygonal model mesh, based on electrode distribution and architectural drawings, to account for the presence of the arches below the bridge. To assess the importance of this step we compare our final results with results computed using an identical inversion set-up calculated on an unstructured rectangular model mesh, as illustrated in Figure 7. While the top $\sim$0.5 m of modelled resistivity beneath the bridge deck is reasonably consistent in structured/unstructured mesh outputs (areas highlighted in green on Figure 7), below this results vary considerably. It might be intuitively assumed that the inversion would automatically identify a high resistivity region in the position of the arch. However, while this does occur to a certain extent (e.g. 10–22.5 m along the southern transect and 12.5–17.5 m along the northern transect in unstructured models, Figure 7b and d) the limited resolution of data at greater depths, is not sufficient for this structure to be naturally identified with well-constrained dimensions. Instead high resistivity values are smeared over a wide region. This results in the masking of more subtle anomalies on the underside of the arches which are visible in the geometric mesh results (areas highlighted in magenta on Figure 7). Given these

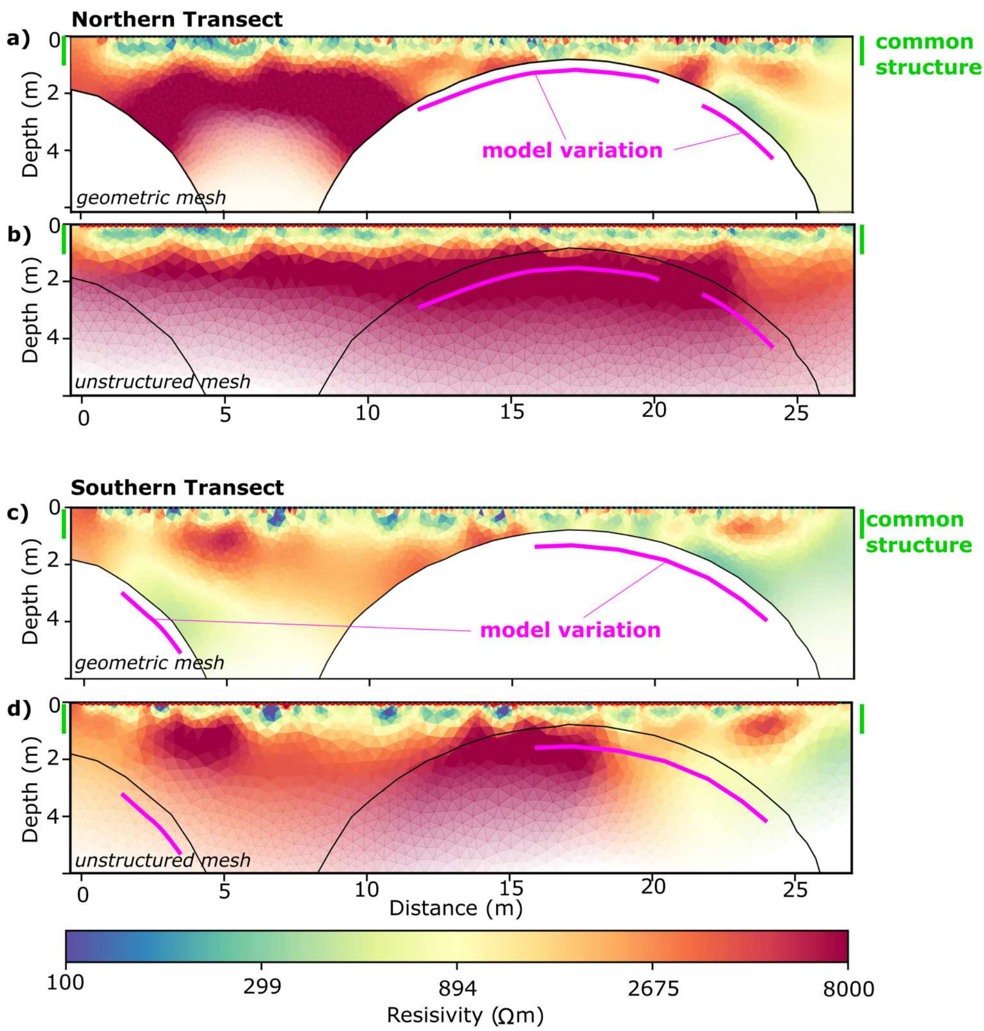

Figure 7. Results of modelled resistivity of material along the norther and southern transects on, a and c – meshes accounting for bridge geometry, and b and d – unstructured rectangular meshes. Areas of common results using either mesh input are highlighted in green, while areas of the models showing variations are highlighted in magenta.

anomalies correlate with observable surface features, they are considered robust results, which are not resolvable without implicit consideration of arch geometry.

To our knowledge there is only one previous study exploring the use of ERT on a heritage bridge:[30] conducted a survey over a small-scale (9 m long, 3.5 m wide) single arch medieval stone bridge, the Pont de Coq, in Normandy, France, with the aim of characterising the road structure. While this study did not directly account for the bridges 3D geometry in model set up (utilising a 2D rectangular grid), they account for its affect by defining areas of the model a priori, with the area under the arch constrained to a high resistivity value representative of air. Theoretically this work-around should have a similar effect on inversion results as designing model boundaries based on geometry. However, given the ease of prescribing a set geometry (at least in 2 dimensions) in standard open-source inversion software, we feel this method is optimal.

5.2. Further development potential for monitoring heritage bridges

Our case study of Prebends Bridge demonstrates clear potential for the application of electrical imaging of heritage masonry bridges on a large scale. Here we explore ways this method could be developed further in the future.

Automated data collection and Temporal monitoring. We found that using an off-the-shelf automated multiplexer instrument such as the TIGRE array, was surprisingly more time intensive in terms of data collection, compared to manual use of four electrodes position using a PSD, connected to a simple Terrameter instrument. However automatic data collection has the potential to be significantly more efficient, though is likely to require design of bespoke equipment. This would need to include a multiplexer cable, connected to a large number of static medical electrical pads, which could be called on in different combinations based on an algorithm run by a simple computing device such (e.g. a low cost raspberry-Pi).

A static electrode setup also opens the possibility for longer-term temporal monitoring, with repeat readings taken over the same transect in varying weather conditions. The use of this approach has been clearly demonstrated on a small scale (several meters)[31, 32] that use ERT to monitor heritage walls over the courses of several hours – up to ~1 d. Data collected in this way can be used to image water drainage patterns as they propagate through features, and subsequent drying patterns during and after weather events. Innovative new technology such as the PRIME (Proactive Infrastructure Monitoring and Evaluation) system,[33] allows near-real-time repeat ERT with remote automated data transfer, has potential to provide long term monitoring of deterioration processes on heritage structures. However logistical constraints may preclude such approaches on bridges (like Prebends) that still accommodate heavy foot/road traffic, given this would require closing off public access to a reasonably large area for extended periods.

Consideration of geometry and electrode placement in three dimensions. In some areas of our results we image low-resistivity (damp) areas at the base of the arch, which do not have a clear connection to the bridge deck, potentially indicating the importance of 3D flow within Prebends Bridge. Placing electrodes in a gridded systems as opposed to straight line transects, has the potential to assess this. This can be carried out using a series of parallel linear transects modelled in 2D with resulting models stitched together, or through using full 3D modelling.[34] On Prebends Bridge, we were spatially limited in terms of extending our linear transects into a gridded system, by the tarmacked surface of the central roadway, where extremely high contact resistance makes data collection impossible. However, another option available on bridge structures would be the placement of additional electrodes on the underside of arches and along bridge sides, in addition to the bridge surface. For most ERT studies, which generally image the subsurface, electrode placement is inherently restricted to data collection at the top of a model. However the potential for 2D electrode positions placed on opposites sides of a built structure, and 3D cross-borehole electrode placements on either side of a wall, has been explored in a desk-based modelling study[35] and in a lab experiment, respectively.[36]

Direct interpretation of moisture for moisture content. In this study, we present maps of variable resistivity, and assume that low-value anomalies represent wet regions; an interpretation supported by the presence of observable external features. However in scenarios where it is possible to get access to direct samples of the imaged material, lab based experiments can be used to quantify the electrical properties of the material under different controlled moisture (and temperature) conditions.[37] This can facilitate a direct interpretation of what different values of resistivity represent in terms of moisture content. While this becomes more difficult in the presence of varying material types (such and the sandstone masonry and sediment back-fill material used in the construction of Prebends Bridge), it is still possible given a good understanding of the spatial distribution of material types, as demonstrated by[38] in their ERT monitoring of a railway cutting, using a well-defined 3D ground model constrained by borehole data. Thus in built structures, this could be achieved where detailed structural plans are available.

6. Conclusions

Geophysical electrical imaging has the potential to provide a powerful tool in monitoring water-induced deterioration of heritage masonry bridges over a large-scale, that can be used to inform intervention strategies and test the effectiveness of those applied. To explore the practicalities of this we conducted a test-study electrical survey on Prebends Bridge in Durham, NE England:

- Two 25 m long transects were taken over the northern and southern sides of the bridges eastern-most arch, which show external visual evidence of water damage.
- Electrical resistivity data was manually collected from measurements on the bridge deck, using a Terrameter instrument and flat metal electrodes covered with electrolyte gel
- Data was modelled using open-source inversion software PyGymli,[39] on a 2D structured mesh honouring the bridges geometry
- This produced models of variable electrical properties within the bridge with sensitivity down to ~3 m
- Low resistivity areas within models are interpreted to represent a near-continuous region of saturated back-fill material in the top 0.5 m, and deeper areas of wet sandstone masonry on the underside of bridge arches
- Model results are consistent with surface features of damp/water staining

- Results suggests water infiltrates though broken flagstones/kerbstones, layers of internal waterproofing built into the structure are ineffective, and concreted repairs to the underside acting only to divert water around repaired sections.

This work demonstrates the effectiveness of electrical imaging on heritage structures on a large-scale context, which requires simple but important adaptions to standard survey techniques. This includes the use of non-destructive electrodes; we find in larger scale surveys requiring the movement of electrodes during data collection, flat base electrodes coated with electrolyte gel are more effective than medical electrical pads. Consideration of bridge geometry (through use of realistic 2D model meshes) is of key importance for imaging more subtle deep internal features, though extension to 3D modelling, does not appear necessary in bridge settings with reasonably planar sides.

While this method is limited to non-tarmacked areas (where high surface resistivity makes data collection impossible), there is scope for significant development of this type of non-destructive imaging. This could include use 3D electrode placement, both in terms of 2D gridded measurements on the bridge deck, as well as additional measurements on arch undersides. Long-term temporal monitoring through repeat surveys along the same transects could also prove effective in imaging water propagation and drying during weather events, and to monitoring long term deterioration. However logistical constraints may make this difficult for bridges still in active use.

Notes

1. E. Martinho and A. Dionísio, 'Main geophysical techniques used for non-destructive evaluation in cultural built heritage: a review', *Journal of Geophysics and Engineering* 11 (2014): 053001.
2. Historic-England, *National heritage list: Prepends bridge listing 1121354* (2024). Available at https://historicengland.org.uk/listing/the-list/list-entry/1121354.
3. D. Brown, *Durham Cathedral: history, fabric and culture*, Yale University Press, 2015.
4. A. March, *Prebends Bridge, bridge deck investigation* (2010), Internal Report commissioned by Durham Cathedral, Unpublished.
5. The Morton Partnership Ltd., *Structural assessment report of Durham Cathedral – Prebends Bridge* (2021), Internal Report commissioned by Durham Cathedral, Unpublished.
6. K. Haelterman, A. Lambrechts, H. Janssens, and D. Van Gemert, 'Geo-electrical survey of masonry', *Materials and structures* 26 (1993): 495–499.
7. D. Van Gemert, H. Janssens, and F. Van Rickstal, 'Evaluation of electrical resistivity maps for ancient masonry', *Materials and Structures* 29 (1996): 158–163.
8. G. Leucci, R. Cataldo, and G. De Nunzio, 'Assessment of fractures in some columns inside the crypt of the cattedrale di otranto using integrated geophysical methods', *Journal of Archaeological Science* 34 (2007): 222–232.
9. N.A. Zeid, M. Balducci, F. Bartocci, R. Regni, and G. Santarato, 'Indirect estimation of injected mortar volume in historical walls using the electrical resistivity tomography', *Journal of Cultural Heritage* 11 (2010): 220–227.
10. O. Sass and H. Viles, 'Wetting and drying of masonry walls: 2d-resistivity monitoring of driving rain experiments on historic stonework in Oxford, UK', *Journal of Applied Geophysics* 70 (2010): 72–83.
11. O. Sass and H. Viles, 'How wet are these walls? testing a novel technique for measuring moisture in ruined walls', *Journal of Cultural Heritage* 7 (2006): 257–263.
12. Zeid et al., 'Indirect estimation'.
13. Leucci et al., 'Assessment of fractures'.

14. Sass and Viles, 'Wetting and drying of masonry walls'.
15. Sass and Viles, 'How wet are these walls?'.
16. C. Fauchard et al., 'Assessment of an ancient bridge combining geophysical and advanced photogrammetric methods: Application to the Pont de coq, France', *Journal of Applied Geophysics* 98 (2013): 100–112.
17. L. Mol and H. Viles, 'Exposing drying patterns: using electrical resistivity tomography to monitor capillary rise in sandstone under varying drying conditions', *Environmental earth sciences* 68 (2013): 1647–1659.
18. Sass and Viles, 'How wet are these walls?'.
19. C. Rücker, T. Günther, and F.M. Wagner, 'pyGIMLi: An open-source library for modelling and inversion in geophysics', *Computers and Geosciences* 109 (2017): 106–123, Available at https://www.sciencedirect.com/science/article/pii/S0098300417300584.
20. The Morton Partnership Ltd., *Structural assessment report of Durham Cathedral*.
21. A. March, *Prebends Bridge*.
22. L. López-González, M. Gomez-Heras, R.O.O. de Cosca, S. Garcia-Morales, and R. Fort, 'Coupling electrical resistivity methods and GIS to evaluate the effect of historic building features on wetting dynamics during wind-driven rain spells', *Journal of Cultural Heritage* 58 (2022): 209–218.
23. R. Flint, P. Jackson, and D. McCann, 'Geophysical imaging inside masonry structures', *NDT & E International* 32 (1999): 469–479.
24. Sass and Viles, 'How wet are these walls?'.
25. Sass and Viles, 'Wetting and drying of masonry walls'.
26. Mol and Viles, 'Exposing drying patterns'.
27. Van Gemert et al., 'Evaluation of electrical resistivity maps'.
28. Ibid.
29. Rücker et al., 'pyGIMLi'.
30. Fauchard et al., 'Assessment of an ancient bridge'.
31. Sass and Viles, 'Wetting and drying of masonry walls'.
32. López-González et al., 'Coupling electrical resistivity methods'.
33. J. Holmes et al., 'Four-dimensional electrical resistivity tomography for continuous, near-real-time monitoring of a landslide affecting transport infrastructure in British Columbia, Canada', *Near Surface Geophysics* 18 (2020): 337–351.
34. L. Capozzoli, G. De Martino, M. Polemio, and E. Rizzo, 'Geophysical techniques for monitoring settlement phenomena occurring in reinforced concrete buildings', Surveys in Geophysics 41 (2019): 575–604.
35. Flint et al., 'Geophysical imaging'.
36. F. Van Rickstal, D. Van Gemert, R. Keersmaekers, and D. Posen, '*Enhancement of geo-electrical techniques for NDT of masonry', in Proceedings of the 6th international conference on structural analysis of historic construction*. 2008, 2–4.
37. Sass and Viles, 'Wetting and drying of masonry walls'.
38. J. Holmes et al., '4d electrical resistivity tomography for assessing the influence of vegetation and subsurface moisture on railway cutting condition', *Engineering Geology* 307 (2022): 106790.
39. Rücker et al., 'pyGIMLi'.

Acknowledgements

LJ acknowledges support of NERC for the undergraduate placement scheme. The authors acknowledge help of high school intern Lara van Hunen who assisted in data collection. We thank Durham Castle and Cathedral World Heritage Site for providing site access and background information, and Historical England for granting the section 42 license. Author contributions are as follows: LF conducted a first survey, inversions and modelling and wrote a preliminary report under supervision of SN, demonstrating feasibility. LJ conducted the main survey, modelling and

inversions, and co-wrote the manuscript. JJ co-wrote the manuscript, co-supervised LJ and contributed to the result modelling and interpretation. SN provided the original idea, designed the acquisition electrodes, supervised LF and LJ, wrote the NERC placement project, adapted the initial pyGIMLi inversion code, contributed to the result modelling and interpretation and co-wrote the manuscript.

Disclosure statement

No potential conflict of interest was reported by the author(s).

Funding

This work was supported by Natural Environment Research Council [Research Experience Placement Scheme].

Notes on contributors

L. Jones has studied Chemistry and Physics and obtained a MSc in Natural Sciences from Durham University in 2024. In the summer of 2023, he conducted research related to this paper thanks to a NERC undergraduate research placement scheme. He will start a PhD on small organic crystallography in September 2024.

J. Jenkins is an Assistant Professor at Earth Sciences, Durham University. Her research interests mainly lie in an observation-driven approach and seismology to better understand deep Earth structure from crustal to mantle scales. Recent work of Dr. Jenkins is expanding into near-surface geophysics applied to a variety environmental problem.

L. Foltier obtained a BSc from Durham University in 2023, after studying geophysics at the Earth Sciences department.

S. Nielsen is a Professor at Earth Sciences, Durham University. He investigates earthquake rupture using laboratory experiments, structural geology and numerical modelling. In recent years he has diversified his interests to include near-surface geophysics for the exploration of underground archaeology, groundwater flow and masonry structures.

ORCID

S. Nielsen http://orcid.org/0000-0002-9214-2932